ISSN 2348 – 9928
IJAICT Volume 2, Issue 12, April 2016 Doi:01.0401/ijaict.2016.12.02 Published on 05 (05) 2016

SPEED CONTROL OF BLDC MOTOR USED IN ANTILOCK BRAKING SYSTEM USING PSO TECHNIQUE

Ms. C. Yamunadevi
PG Scholar,
Nandha Engineering College,
Erode, Tamilnadu, India.

Ms. A. Rajeswari
Assistant Professor,
Nandha Engineering College,
Erode, Tamilnadu, India.

Abstract – This paper proposes a design of optimal PI(D) controller for brushless DC (BLDC) motor speed control by the particle swarm optimization (PSO), one of the powerful metaheuristic optimization search techniques. The proposed control system is implemented on the TMS320F28335 DSP board interfacing to MATLAB/SIMULINK. With Back EMF detection, the proposed system is considered as a class of sensorless control. This scheme leads to the speed adjustment of the BLDC motor by PWM. In this work, the BLDC motor of 100 watt is conducted to investigate the control performance. As results, it was found that the speed response of BLDC motor can be regulated at the operating speed of 800 and 1200 rpm in both no load and full load conditions. Very satisfactory responses of the BLDC system can be successfully achieved by the proposed control structure and PSO-based design approach.

Keywords – BLDC Motor, PI(D) Controller, Particle Swarm Optimization, Back EMF Detection.

I. INTRODUCTION

The antilock braking system (ABS) is a crucial safety system in modern vehicles. The role of the ABS is to maintain the steerability of the vehicle while trying to minimize the vehicle stopping distance in panic braking or challenging braking scenarios. In the last two decades, numerous attempts have been made to improve the performance of ABSs for conventional vehicles. As a result of using advanced control methods, the performance of ABS for conventional frictional brakes is close to optimal (see [1]–[3], [6], and references therein). On the other hand, issues related to the design of ABSs for electric vehicles (EVs) have recently gained attention [7], [8], and the problem of designing ABSs for in-wheel EVs is yet to be investigated. In EVs that use the in-wheel design, a separate electric machine is available at each corner of the vehicle. These independent electrical machines provide unique opportunities for enhanced control strategies of the vehicle. The availability of an electric machine at each corner of EV provides an additional degree of freedom in the design of the vehicle braking system as well. One approach is to use the regenerative back electromotive force (EMF) of the electric machine to recharge the EV batteries and produce regenerative braking torque to improve the performance of the braking system. However, in almost all existing EVs, it is common to disengage the regenerative braking torque during activation of ABSs and decelerate the vehicle entirely by the frictional braking torque [2]. The energy harvest during ABS activation cannot be economically justified as the ABS is rarely activated or is activated only for a very short time. The introduction of the additional regenerative braking torque could complicate the ABS control strategy and risks the safety of the vehicle. However, the regenerative back EMF of each in-wheel motor can still be effectively exploited to enhance the ABS of in-wheel EVs.

Recently, a sensor less ABS was introduced in [2], [3] and simulation results in the paper showed that the back EMF of a *brushed* in-wheel EV can be used to estimate wheel speed and identify road condition in real time. An accurate wheel speed measurement system for sensorless ABS of a *brushed in*-wheel EV was realized in [7]. A more in-depth explanation of the above sensorless ABS was given in [8], which compared results of sensorless wheel speed estimations with measurement results of an actual ABS sensor. It was shown that thesensorless ABS introduced in [6]–[8] estimates the wheel speed with higher accuracy compared with ABS sensors and omits the need to install separate ABS sensors at each corner of the vehicle. The assumption underpinning this approach is that the regenerative back EMF can be used to simplify and improve the *wheel speed measurement* part of the ABS. This means that other parts of the ABS, including its controller, remain intact and the ABS standard or advanced control strategies that have been fully tested for many years and are legally approved can still be utilized. The above sensorless ABS was solely considered for *brushed*-dc-motor-driven in-wheel Evs. A brushed permanent magnet dc motor has a very simple dynamic: Its back-EMF analysis is

ISSN 2348 – 9928
IJAICT Volume 2, Issue 12, April 2016 Doi:01.0401/ijaict.2016.12.02 Published on 05 (05) 2016

straightforward, and its efficiency and maintenance requirement are suboptimal due to the use of brushes for commutation. On the other hand, in-wheel EVs require motors withhigh efficiency and low maintenance for their propulsion system.

As a result, brushless motors have gradually become the number one choice for almost all in-wheel EVs [15]. This is despite the fact that the dynamics of brushless motors is more complicated than the brushed motors and therefore their back-EMF outputs are significantly different. In this paper, we investigate the feasibility of developing a sensorless ABS for brushless-motor - driven in-wheel EVs that would significantly reduce their maintenance and final cost and simplify their design. We will show that the back EMF of brushless motors, despite their complicated patterns, can be used to measure the wheel speed with similar (or better) accuracy compared with commercial ABS sensors and sensorless wheel speed measurement using brushed dc motors.

II. BLDC MODEL AND DSP BOARD

2.1 BLDC Model

In practice, the commutation of the brushless DC motor is done electronically. The position of rotor is very important for electrical commutation. Usually, the Hall sensors are placed in 120-degree intervals and the common operation of BLDC motor is achieved by six-section.

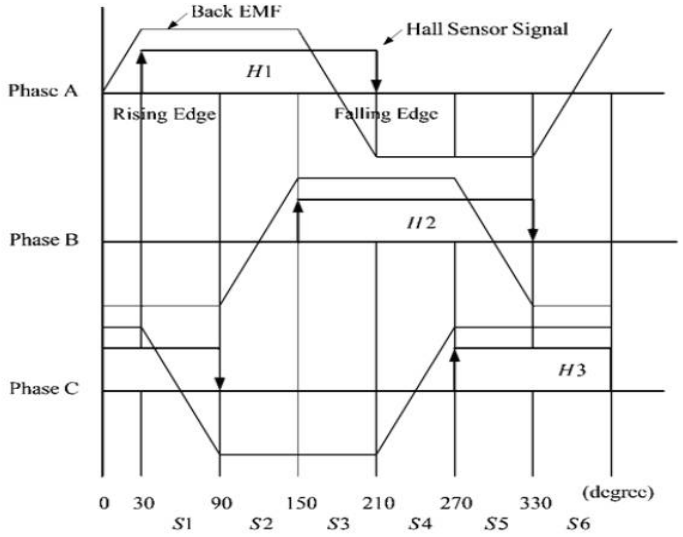

Fig 1 : Back EMF and Hall effect sensor signals

The Back EMF and Hall sensor signals are depicted in Fig. 1. Once the magnetic poles of rotor come to Hall sensor, the sensory signals are generated. According to the six-step in Fig. 1, the commutation sequence is performed. The motor phases are supposed to conduct for 120 electrical degrees two times per cycle. The two phases are only conducted at one time. The Hall sensor signal has the rising and falling edges for each phase. This means that the sixtrigger signals are generated per one cycle. Using these trigger signals, motor control is carried out. The switching sequence for commutation phase is given in Table 1. For forward and reverse directions of rotor, switching sequence is different.

TABLE 1: SWITCHING SEQUENCE

Directions	Switching sectors					
	S1	S2	S3	S4	S5	S6
Forward	a^+b^-	a^+c^-	b^+c^-	b^+a^-	c^+a^-	c^+b^-
Reverse	b^+a^-	c^+a^-	c^+b^-	a^+b^-	a^+c^-	b^+c^-

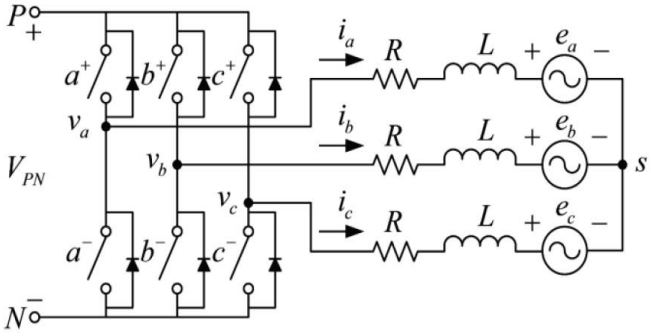

Fig 2 : Equivalent circuit of BLDC Motor

Modeling of BLDC motor is similar to three-phase synchronous machine. Since there is permanent magnet mounted on the rotor, some dynamic characteristics are different. Model of BLDC motor can be formulated through the electrical equivalent circuit represented in Fig. 2 [9-12].

2.2 Back EMFs Sensing

However, the back EMFs cannot directly be detected and, hence, should indirectly be obtained. Thus, by proper transformation, the ZCPs of back EMFs can be obtained from *ux*. Here, take phases A and B conducting as an example to analyze this detection method. At this time, the amplitudes of the back EMFs for the conduction phases during each commutation state are equal, and their polarities are opposite, i.e., *ea*+ *eb*= 0. Moreover, because the armature of phase C is disconnected from the voltagesources, the terminal voltage of phase C can be expressed as the summation of the armature back EMF and the neutral voltage, i.e.,

$$uc = ec + un. \quad (1)$$

Because $ia = -ib$ and $ic = 0$

$$un = 1/2\,(ua + ub). \quad (2)$$

Substituting (2) into (1), we will have the following ZCP detection equation:

$$ec = uc - 1/2\,(ua + ub). \quad (3)$$

As aforementioned, it is easy to obtain the back EMF equations of phases A and B as $ea = ua - 0.5(ub + uc)$ and $eb = ub - 0.5(ua + uc)$, respectively. From these equations, the computation of back EMFs *ea*, *eb*, and *ec*do not require neutral voltage *un*; thus, the ZCPs of back EMFs can directly be extracted from *ua*, *ub*, and *uc*. As shown in Fig. 2, if the ZCPs of *ea*, *eb*, and *ec*are obtained, then by delaying 30 electric degrees, the commutation points can be obtained.

Based on the aforementioned detection principle, the designed detection circuit of back EMFs is shown in Fig. 1. Because the PWM technique is adopted, the terminal voltages contain rich high-frequency components; thus, the neutral voltage varies with the motor speed. To eliminate the effect of a motor neutral point, the virtual neutral point *N* of detection circuit is taken as the reference point and is connected to the ground of the detection circuit instead of the source cathode.

Thus, the reference voltage *ur*of the comparator would not fluctuate with the motor speed and remains unchanged in spite of varying speed. After the dividing and filtering process, voltages *uao*, *ubo*, and *uco*are compared with *ur*, and zero-crossing signals *uaz*, *ubz*, and *ucz*can be obtained. With these signals, sensor-less commutation control is then achieved.

2.3 DSP Controller Board

The DSP controller board used in this work is the Texas Instrument TMS320F28335 [4] consisting of a 32-bit CPU and a single-precision 32-bit floating-point.

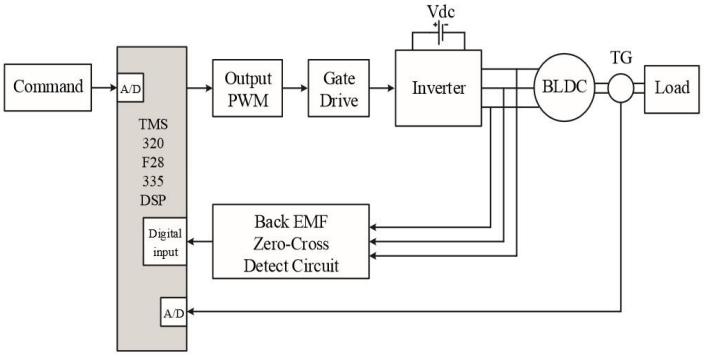

Fig 3 : DSP based speed control of BLDC motor

The 150 MHz system clock is provided by an on-chip oscillator including the MATLAB/SIMULINK software platform [5]. The module board includes 3-phase PWM inverter 90V, 5A upto 25 kHz PWM frequency and measurement of motor currents in all 3 phases with DC voltage supply of 5Vdc.

The BLDC motor speed control system based on TMS320F28335 DSP board can be represented in Fig. 3. The MATLAB/SIMULINK platform is integrated to monitor communication program and DSP applications. Using the PC communication module, it can accessible to the TMS320F28335 DSP controller board and execute any application program in order to analyze and evaluate the overall system performance.

III. PSOALGORITHM AND PI(D)DESIGN PROBLEM

3.1 PSO Algorithm

The general idea Control (PSO) is to create a closed loop controller with parameters that can be updated to change the response of the system. The output of the system is compared to a desired response from a reference model. The control parameters are update based on this error. The goal is for the parameters to converge to ideal values that cause the plant response to match the response of the reference model. For example, you may be trying to control the position of a robot arm naturally vibrates. You actually want the robot arm to make quick motions with little or no vibration. Using PSO, you could choose a reference model that could respond quickly to a step input with a short settling time.

The algorithm is initialized with particles at random positions, and then it explores the search space to find better solutions. In every iteration, each particle adjusts its velocity to follow two best solutions. The first is the cognitive part, where the particle follows its own best solution found so far. This is the solution that produces the lowest cost (has the highest fitness). This value is called pBest (particle best). The other best value is the current best solution of the swarm, i.e., the best solution by any particle in the swarm. This value is called gBest (global best). Then, each particle adjusts its velocity and position with the following equations:

$$v' = v + c1.r1.(pBest - x) + c2.r2.(gBest - x) \quad (4)$$

$$x' = x + v' \quad (5)$$

where v is the current velocity, v' is the new velocity, x is the current position, x' is the new position, pBest and gBest as stated above, r1 and r2 are even distributed random numbers in the interval [0, 1], and c1 and c2 are acceleration coefficients. Where

c1 is the factor that influences the cognitive behaviour, i.e., how much the particle will follow its own best solution, and c2 is the factor for social behaviour, i.e., how much the particle will follow the swarm's best solution.

The algorithm can be written as follows:

(i) Initialize each particle with a random velocity and random position.
(ii) Calculate the cost for each particle. If the current cost is lower than the best value so far, remember this position (pBest).
(iii) Choose the particle with the lowest cost of all particles. The position of this particle is gBest.
(iv) Calculate, for each particle, the new velocity and position according to the above equations.
(v) Repeat steps ii-iv until maximum iteration or minimum error criteria is not attained.

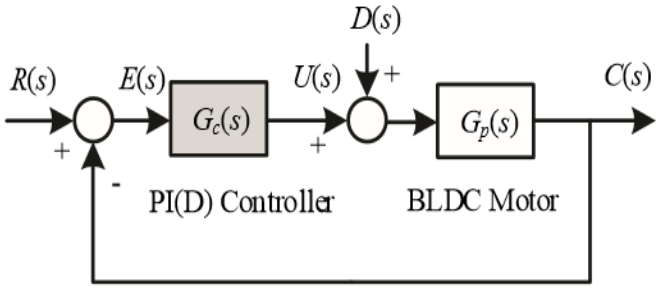

Fig 4 : PI(D) control loop

3.2 PSO-based PI (D) Design Problem

The use of proportional-integral (PI), proportional-integralderivative (PID) controllers for industrial applications was first introduced in 1939 [13, 14]. Due to ease of use and simple realization, PI-PID controllers have been increasingly employed in the control system over decades. The PI(D) control loop can be represented by the block diagram in Fig. 4. The PI(D) controller receives the error signal, E(s), and generates the control signal, U(s), to regulate the output response, C(s), referred to the input, R(s) and to reject the disturbance signal, D(s), where Gp(s) and Gc(s) are the plant and the controller transfer functions, respectively.

In this work, the PSO is applied to design an optimal PI(D) controller in order to gain the optimal response of the BLDC system. The PSO-based PI(D) controller design for BLDC system can be represented by the block diagram in Fig. 5, where C(s) and C*(s) stand for actual and desiredresponses.

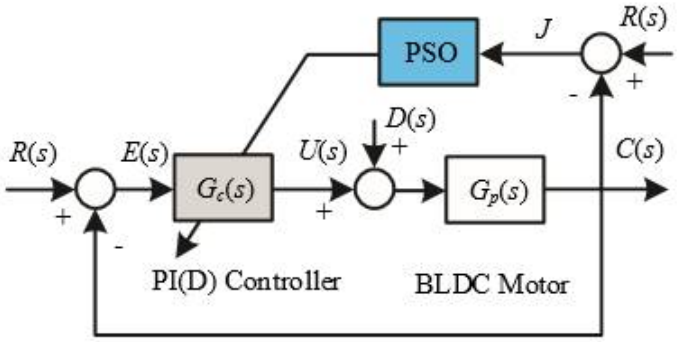

Fig 5 : PSO based PI(D) controller design

IV. ELECTRIC BRAKE SYSTEM

The proposed electric braking system involves three modes: the regenerative brake, kinetic brake, and short-circuit brake mechanisms. The braking controller must adjust the brake torque by changing the time ratio between the short–circuit and kinetic brakes for maintaining the optimal slip ratio and avoiding the vehicle wheels from locking and skidding. To demonstrate, the different actuation principles of the three brake modes are mathematically formulated below.

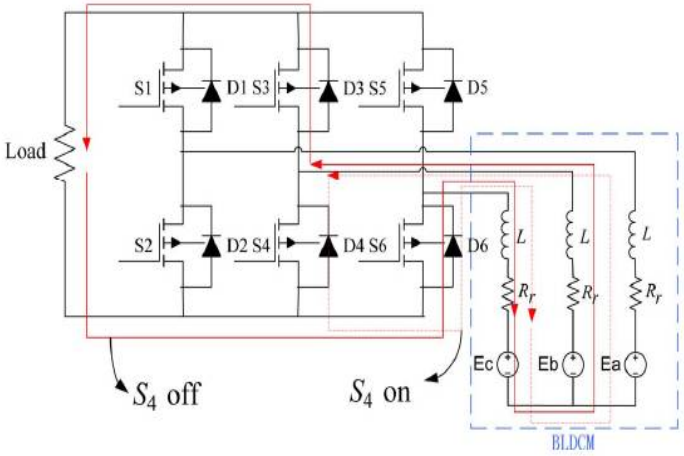

Fig 6 : Current conduction loop in short-circuit and kineticbrakemode, which correspond to S4 on and S4 off, respectively.

Short-Circuit Brake: The short-circuit brake aims at producing the largest brake force among the three brake modes. For this mode, the load in Fig. 3 is treated as zero electrical resistance such that $Vap - Vbp = Rr(iap - ibp) + Ld(iap - ibp)/dt$by using Kirchhoff's voltage law where (iap, ibp) and (Vap, Vbp) are phase current and voltage of the short-circuit brake, respectively. The brake torque is further given by

$$Tb = Kt(iap - ibp) \quad (6)$$

since it is proportional to the input current of BLDCM.

Regenerative Brake: The regenerative brake is capableof converting kinetic energy to electric energy, which is generated by the driving motors and further recharged to the battery, which is treated as the load in Fig. 6 so that $Vap - Vbp = Rr(iap - ibp) + Ld(iap - ibp)/dt + Vbat$uponKirchhoff's voltage law where $V_{bat}$is the battery voltage. The desired brake torque is also described by (15).

Kinetic Brake: The kinetic brake is aimed at directing electric energy to a high-power resistor which serves as the dummy load *RL* to the electric energy generator. Given *RL* as the load in Fig. 3, the mathematical model is described as $Vap - Vbp = R(iap - ibp) + Ld(iap - ibp)/dt + RL(iap - ibp)$ based on Kirchhoff's voltage law. The corresponding brake torque is generated as (15).

4.1 Analysis of the Braking Mode for the Driving Motor

The proposed electric brake utilizes the back EMF as the power source, which is generated by the BLDCM in braking. Moreover, the kinetic energy is converted to electric energy via the feedback current of the dummy load upon a rectifier circuit, adjusting the brake torque according to PWM signals. To illustrate, Fig. 6 illustrates the current conduction for the short-circuit brake and kinetic brake modes; it shows that:

1) the short-circuit loop has the current, generated by the motor and flowing through S4, D6, and two motor phases when *S*4 is on;

2) at the same time, returning the feedback current to the motor's inductor generates the effect of short-circuit brake; and 3) the kinetic energy of the motor is directed to the dummy load by the kinetic brake, resulted by the current flowing through D3 and D6 while *S*4 is off. This yields the smaller brake torque while comparing to that of the short-circuit brake mode.

As for the boundary layer speed control, the controller keeps the vehicle speed within the optimal range which is related to the safety range of the slip ratio by adjusting brake force upon the flow chart in Fig. 7 while the vehicle speed lies out of the desired range and the slip ratio is larger than the previous one. In Fig. 9, *BS* is boundary layer speed, *BFv*and *BFω*are brake torques added to the wheels revealing faster and slower speeds, respectively, and *BFf*and *BFr*are percentages of the brake forces corresponding to the front and rear wheels.

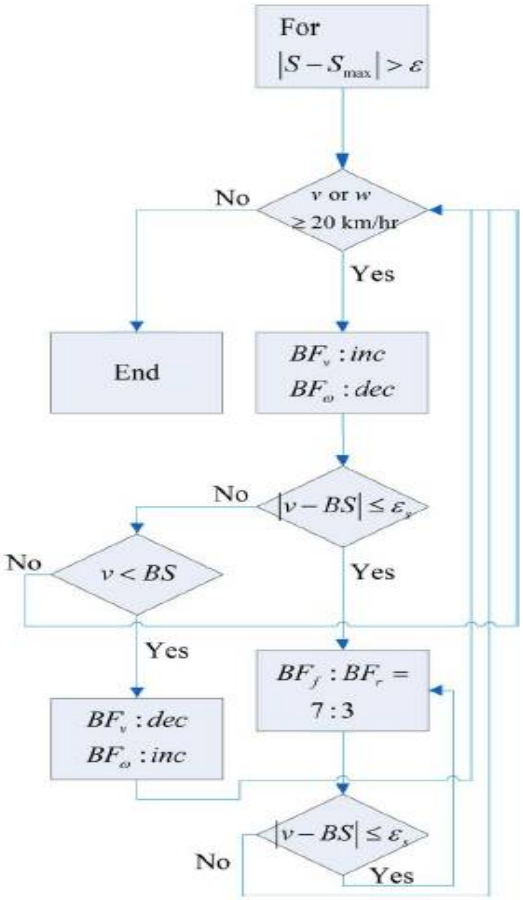

Fig 7 : Flow chart of the adjustment for the brake forces.

4.2 Adjustment of Brake Force

System stability in the vehicle braking requires the guarantee of the optimal slip ratio; therefore, the distribution regulation of the brake forces for achieving effective braking performance becomes an important issue. Since relevant papers have proved that change of vehicle's inertia causes extra load to the front wheel, the braking system in our case adjusts the brake force ratio to 7 : 3 on the front and rear wheels.

The flow chart in Fig. 7 is performed by four steps. First, the controller calculates the slip ratio and adjusts the brake torques if $|S - S\max| > \varepsilon$ and the wheel speed is larger than 20 km/h; otherwise, the process is ended. Second, if $|v - BS| \le \varepsilon s$, the ratio of brake torques is adjusted to 7 :3 on the front and rear wheels. Third, the brake torques—imposed on the two wheels vary according to the control gain if $v < BS$ and $|v - BS| > \varepsilon s$. Last, if the wheel speed is smaller than 20 km/h, the controller inhibits the action of ABS and adopts the maximum brake torque instead

such that the ES stops in the shortest time. Otherwise, the process returns to the first step.

V. SIMULATION RESULTS

Regarding to Fig. 5, the PSO is applied to design the PI(D) controller for the BLDC system. The PSO algorithm is coded by MATLAB running on Intel Core2 Duo 2.0 GHz 3 Gbytes DDR-RAM computer. For this application, the number of particles is set of 100. c1 = c2 = 2.0, r1 and r2 are random numbers uniformly distributed in the range [0, 1], wmin = 0.4, wmax = 0.9 and kmax = 1,000 is maximum iteration set as the termination criteria for each trial. For comparison, the GA and TS are conducted to design the PI(D) controller for the BLDC system. Search parameters of the GA and TS are set as the original ones. Both GA and TS will be terminated when the generation or iteration reaches 1,000. Algorithms of the GA and TS are omitted. Readers can find the details of GA in [16-17] and TS in [18-20], respectively. Those algorithms are coded byMATLAB running on the same platform. For the PI controller design, the boundaries of the PI parameters are set to perform the search space as follows: Kp∈ [0, 10] and Ki ∈ [50, 100]. The design performs the search of 50 trials with different initial solutions in order to obtain the best solution. Referring to Fig. 8, the system responses of the BLDC motor system and the search time can be summarized in Table 2, where Tr is the rise time, Mp is the maximum percent overshoot, Ts is the settling time and ess is the steady state error. From the Table 2, with the smallest search time consumed the PSO can provide the optimal PIcontroller for the BLDC motor controlled system giving the fastest response with shortest rise time and settling time. For the PID controller design, the boundaries of the PID parameters are set to perform the search space as follows: Kp∈ [0, 10], Ki ∈ [50, 100] and Kd∈ [0, 1]. The design performs the search of 50 trials to obtain the best solution.

TABLE 2: SYSTEM RESPONSESBY PI

Entry	System Responses by PI				Search time (sec)
	Tr (sec)	Mp(%)	Ts(sec)	ess(%)	
GA	0.043	1.823	0.327	0.00	228.14
TS	0.041	3.102	0.216	0.00	165.52
PSO	0.042	4.645	0.126	0.00	76.27

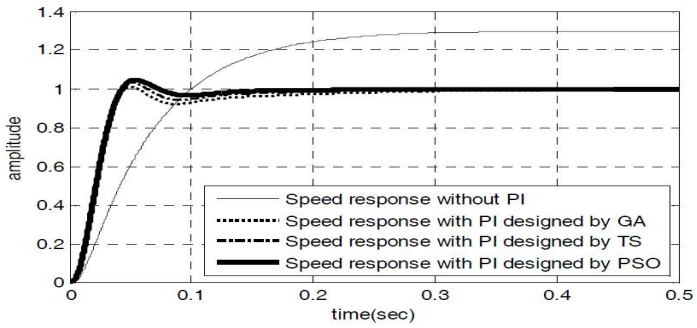

Fig 8 : System responses of BLDC with PI controller designed by GA, TS and PSO

TABLE 3: SYSTEM RESPONSESBY PID

Entry	System Responses by PID				Search time (sec)
	Tr (sec)	Mp(%)	Ts(sec)	ess(%)	
GA	0.028	6.344	0.128	0.00	257.62
TS	0.027	5.982	0.894	0.00	198.17
PSO	0.026	4.281	0.056	0.00	98.48

Referring to Fig. 9, the system responses of the BLDCmotor controlled system and the search time consumed can be summarized in Table 3. From the Table 3, it was found that with the smallest search time consumed the PSO can provide the optimal PID controller for the BLDC motor controlled system giving the fastest response with shortest rise time and settling time as well as smallest overshoot.

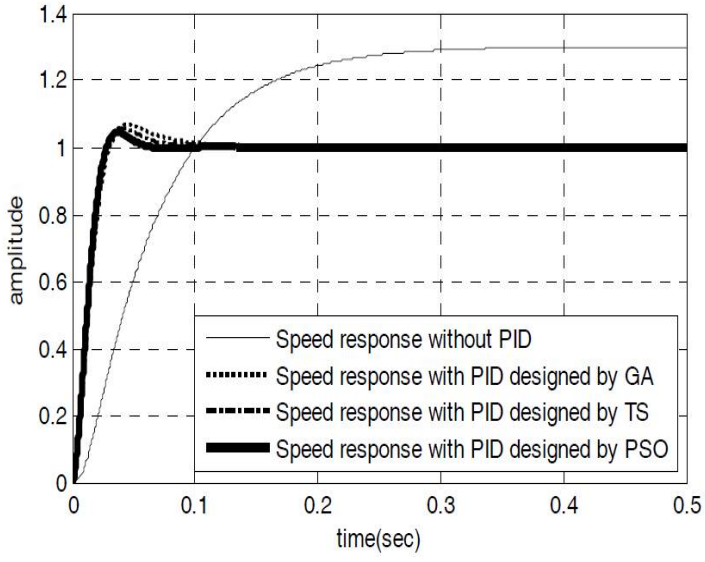

Fig 9 : System responses of BLDC with PI controller designed by GA, TS and PSO

VI. EXPERIMENTAL RESULTS

The BLDC motor speed control system is implemented by using the 100 watt, 2000 rpm BLDC motor as shown in Fig. 10. The speed of motor ranging from 0 to 2000 rpm can be measured by tacho-generator of 0.825V/500 rpm. A speed transformed to be a voltage ranging from 0 to 3.3 V will be sent to A/D convertor. This scheme enables the user can adjust the speed of the motor by the power amplifier. The performance of implemented BLDC motor based on TMS320F28335 DSP board with the MATLAB/SIMULINK can be tested by sampling rate of 0.0001 sec. In this work, the operating speed of 800 and 1200 rpm is specified because this speed range is suitable for designed Back EMF detecting circuit.

TABLE 4: ENTIRE SYSTEM PERFORMANCESBY PI

	System performances by PI controller			
Entry	Tr (sec)	Mp(%)	Ts(sec)	ess(%)
No load	0.045	5.632	0.157	0.00
Full load	0.080	2.546	0.182	0.00

TABLE 5: ENTIRE SYSTEM PERFORMANCESBY PID

	System performances by PID controller			
Entry	Tr (sec)	Mp(%)	Ts(sec)	ess(%)
No load	0.026	4.282	0.057	0.00
Full load	0.028	1.524	0.059	0.00

At lower speed, it is neglected because the performance of the BLDC motor controlled system is decreased due to low level of Back EMF. The reversed direction control is also omitted because it performs the same characteristic (with opposite sign). Therefore, the measurements will be divided into two groups. The first is a step change of the speed reference at constant load torque, while the second is a step change of the load torque at constant speed reference. Speed responses of the system via the step change from 800 to 1200 rpm of speed reference without and with rated load torque are investigated.The experimental results are measured by a digitalstorage scope YOKOGAWA DL1540C in which the ratio of a voltage sensor is 100V/DIV and a current sensor is 2.0A/DIV.

Referring to Table 4, it was found that at the speed from800 rpm to 1200 rpm the system response reaches to desired steady state level. In case of no load, the step response declares values of Tr, Mp, Ts and ess almost as same as the those values obtained from simulation as can be observed in Fig. 8 and Table 2. However, Tr and Ts of the full load is a little bit slower than that of no load condition. Also, Mp of the full load is lower than that of no load condition. At both conditions, the BLDC system responses have no steady state error.

VI. CONCLUSION

Designing an optimal PI(D) controller for brushless DC (BLDC) motor speed control based on the PSO has been proposed in this paper. By using back EMF detection based on TMS320F28335 DSP board, the proposed control structure has been interfaced to MATLAB/SIMULINK. The PSO has been applied to design the PI(D) controller to obtain the optimal tracking and regulating responses. Performance of the proposed system has been evaluated against the BLDC motor of 100 watt. As simulation results comparing with the GA and TS, it was found that with the shortest search time consumed the PSO could provide the optimal PI(D) controller giving the fastest response with shortest rise and settling times as well as smallest overshoot. As experimental results, it was found that the satisfactory tracking and regulating speed response of BLDC motor can be achieved from 800 and 1200 rpm with no load and full load conditions. Experimental results strongly agree to simulation ones. This can be concluded that the proposed design approach and control structure aremost efficient and alternative to control the BLDC motor effectively.

References

[1] A. V. Topalov, Y. Oniz, E. Kayacan, and O. Kaynak, “Neuro-fuzzy control of antilock braking system using sliding mode incremental learning algorithm,” Neurocomputing, vol. 74, no. 11, pp. 1883–1893, May 2011.

[2] R. de Castro, R. E. Araujo, and D. Freitas, “Wheel slip control of EVs based on sliding mode technique with conditional integrators,” IEEE Trans. Ind. Electron., vol. 60, no. 8, pp. 3256–3271, Aug. 2013.

[3] L. Weng-Ching, L. Chun-Liang, H. Ping-Min, and W. Meng-Tzong, “Realization of anti-lock braking strategy for electric scooters,” IEEE Trans. Ind. Electron., vol. 61, no. 6, pp. 2826–2833, Jun. 2014.

[4] TMS320F28335, Digital Signal Controller, Texas Instruments, 2007.

[5] The Math Works Inc., MATLAB/SIMULINK User’s Guide, Natick, MA, 1998.

[6] A. Dadashnialehi, Z. Cao, A. Kapoor, and A. Bab-Hadiashar, “Intelligent sensorless ABS for regenerative brakes,” in Proc. IEEE IEVC, 2012, pp. 1–5.

[7] A. Dadashnialehi, A. Bab-Hadiashar, Z. Cao, and A. Kapoor, “Accurate wheelspeedmeasurementforsensorlessABSinelectricvehicle,”inProc. IEEE ICVES, 2012, pp. 37–42.

[8] A. Dadashnialehi, A. Bab-Hadiashar, Z. Cao, and A. Kapoor, "Intelligent sensorless ABS for in-wheel electric vehicles," IEEE Trans. Ind. Electron., vol. 61, no. 4, pp. 1957–1969, Apr. 2014.

[9] T. J. Sokira and W. Jaffe, Brushless DC motors: Electronic Commutation and Control, Tab Books, USA, 1989.

[10] R. Krishnan, Electric Motor Drives Modeling, Analysis, and Control, Prentice-Hall International Inc., New Jersey, 2001.

[11] P. C. Krause, O. Wasynczuk, S. D. Sudhoff, Analysis of Electric Machinery and Drive Systems, IEEE Press, Piscataway, NJ, 2002.

[12] P. P. Acarnley, J. F. Watson, "Review of positionsensor less operation of brushless permanent-magnet machines," IEEE Trans. Industrial Electronics, vol. 53(2), pp. 352-362, 2006.

[13] N. Minorsky, "Directional stability of automaticallysteered bodies," Journal of the American Society of Naval Engineering, vol. 34, p. 284, 1922.

[14] S. Bennett, "Development of the PID controller," IEEE Control System Magazine, pp. 58-65, 1994.

[15] K.T.Chau,C.C.Chan,andL.Chunhua,"Overviewofpermanent-magnet brushless drives for electric and hybrid electric vehicles," IEEE Trans. Ind. Electron., vol. 55, no. 6, pp. 2246–2257, Jun. 2008.

[16] D. E. Goldberg, Genetic Algorithm in Search, Optimization, and Machine Learning. Addison-Wesley Publishing, 1989.

[17] D. E. Goldberg, "Genetic and evolutionary algorithms come of age," Communication of the ACM, vol. 37(3), pp. 113-119, 1994.

[18] F. Glover, "Tabu search - part I," ORSA Journal on Computing, vol. 1(3), pp. 190-206, 1989.

[19] F. Glover, "Tabu search - part ii," ORSA Journal on Computing, vol. 2(1), pp. 4-32, 1990.

[20] F. Glover, "Parametric tabu-search for mixed integer programs," Journal of Computers and Operations Research, vol. 33, pp. 2449-2494, 2006.